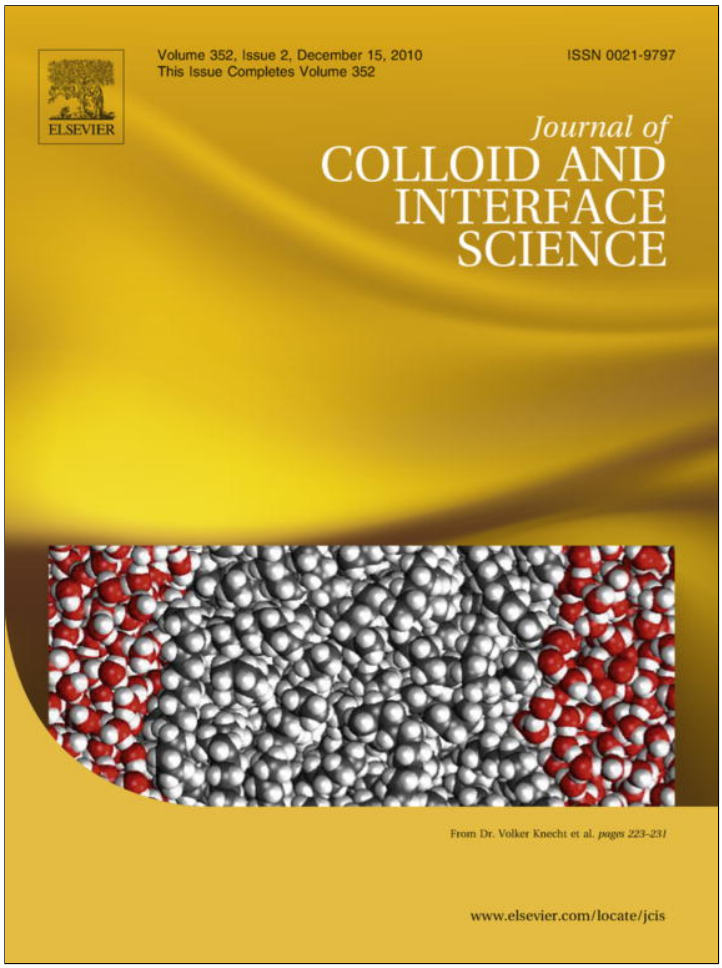

Journal of Colloid and Interface Science 352 (2010) 526–534

Contents lists available at ScienceDirect

Journal of Colloid and Interface Science

www.elsevier.com/locate/jcis

Surface binding site analysis of Ca^{2+}-homoionized clay–humic acid complexes

Raul E. Martinez, Prasesh Sharma, Andreas Kappler *

Geomicrobiology, Center for Applied Geosciences, University of Tuebingen, Germany

ARTICLE INFO

Article history:
Received 3 August 2010
Accepted 28 August 2010
Available online 22 September 2010

Keywords:
Kaolinite
Illite
Humic acid–clay complexes
Surface complexation modeling
FTIR
Zeta potential

ABSTRACT

Clay–humic substance complexes play a major role in controlling the mobility of toxic metals in contaminated soils. However, our understanding of the underlying mechanisms is limited. Binding site analysis of clay and clay–mineral–humic composites, in this study, revealed an enhanced surface reactivity for the clay surface by the sorbed humic substances. Kaolinite and illite had three binding sites with pK_a values ranging from ~4.5 to 9.6 at Ca^{2+} concentrations of 0.01 and 0.1 M respectively. In the presence of peat humic acid (PHA), four or five binding sites were observed for humics sorbed kaolinite surface at Ca^{2+} concentrations of 0.01 and 0.1 M respectively. pK_a values ranged from ~4.4 to 9.6 for humic acid concentration of 0.01 and 0.1 mg/mL. For illite, four or five binding sites were found with pK_as ranging from ~4.1 to 9.4. From zeta potential measurements of PHA-kaolinite or PHA-illite suspensions, the already negative potential decreased by 30 mV from pH 4 to 7, and by 10 mV for pH values greater than 7. For illite the initial negative surface potential decreased by 15 mV up to a pH of 9. Above this pH, the potential decrease diminished to 2 or 5 mV. These changes in surface potential confirm the adsorption of PHA to the clay mineral surface. FTIR measurements of clay samples were able to identify the kaolinite and illite phases. In addition, FTIR absorption bands found in the range of 1950–1800 cm^{-1}, suggest the interaction of PHA with kaolinite and illite surfaces. The results of this study indicate that the sorption of humic substances increases the availability of clay surface functional groups for deprotonation and potential sorption of toxic metal cations.

1. Introduction

Kaolinite and illite are clay minerals that represent major constituents of soils and sediments [1–4]. These are examples of reactive geochemical solids whose interactions with soil organic matter play a key role in the transport of toxic substances [5–9]. Kaolinite has a 1:1 tetraoctahedral aluminosilicate structure with the general formula: $Al_2Si_2O_5(OH)_4$, with two different basal cleavage faces. One face consists of tetrahedral siloxane (—Si—O—Si—) species, while the other of an octahedral, alumina (Al_2O_3) sheet. At the edges of kaolinite particles, octahedral alumina and silica tetrahedral sheets expose reactive functional moieties including aluminol (Al—OH) and silanol (Si—OH) groups. The hydroxyl (—OH) groups can be deprotonated to generate a net negative charge. The edge faces are estimated to occupy approximately 10% of the whole kaolinite surface. The basal face of kaolinite, carries a net negative charge as a result of isomorphous substitution of Si^{4+} by Al^{3+} groups [10–15].

Illite is an aluminum–potassium mica-like, non-expanding, dioctahedral mineral, usually present in the clay fraction. Illite has been described as an interlayer deficient mica and it crystallizes in the monoclinic system, where two tetrahedral sheets sandwich an octahedral sheet. An approximate formula for illite is: $K_{0.88}Al_2(Si_{3.12}Al_{0.88})O_{10}(OH)_2$. In this 2:1 layered system, the illite surface has been proposed to be heterogeneous, with different binding affinities for protons or other ions. The morphology of the illite crystal and the complexity of its surface suggest a number of surface reactive sites, including weakly acidic basal planes and amphoteric silanol and aluminol sites on the edge surface [16–19]. For the most part, however, because of the clay structural complexity and the limited ability of current surface complexation models (SCMs), and optimization routines such those included, for example, in the FITEQL® code [20], to predict the number of reactive sites, two binding sites have been assumed on clay mineral surfaces [16,17,21,22]. In order to better understand the nature of metal and organic matter complexation to clays, not only the number of available sites, but their most accurate apparent pK_a values and concentrations must be first defined. The inclusion of electrostatic parameters enhances the flexibility of optimization routines. This, coupled to the need for a close initial input guess on the number and concentration of sites renders, both the SCM models (which in most cases assume only one or two binding sites)

* Corresponding author. Address: Geomicrobiology, Center for Applied Geosciences, University of Tübingen, Sigwartstrasse 10, D-72076 Tübingen, Germany. Fax: +49 7071 295059.
E-mail address: andreas.kappler@uni-tuebingen.de (A. Kappler).

0021-9797/$ - see front matter © 2010 Elsevier Inc. All rights reserved.
doi:10.1016/j.jcis.2010.08.082

and their respective optimization approaches (e.g. FITEQL® [20]), at the least, questionable. A mathematical fit of experimental data, based on a more flexible model, means that the resulting optimized parameters may not be representative of the system being studied.

Organic coating of the clay surface by sorbed humic substances plays a key role in partitioning and transport of toxic metals in soils. However, very few studies have quantified humic sorption onto the clay surface [4,5,13,23–27]. Humic substances are mixtures of polydisperse, heterogeneous polyelectrolytes [23,28–30]. They are negatively charged due to the presence of carboxylic acid and phenolic groups on aromatic residues and aliphatic chains. The solubility and conformation of humic substances in aqueous media are determined by pH, background electrolyte concentration, and the interaction of the deprotonated functional groups (carboxyl and hydroxyl) with metals and polyvalent cations [1,23,28–30]. For example, Ca^{2+} has been proposed to cause condensation of humic acid molecules. This may increase the amount of humics adsorbed to the clay surface and influence the conformation and orientation of sorbed organic molecules. This process would then dominate the ability of the organic coating and the clay surface to complex trace metal cations in the soil [5,23,26].

Major cations in soils including Ca^{2+}, Mg^{2+}, and Na^{+} are readily sorbed on clay surfaces by ion exchange mechanisms. Clay minerals have also shown a generally ineffective adsorbing of anions, including Cl^{-} and I^{-} [23,31–33]. As mentioned previously, polyvalent cation generated changes in molecular conformation play a key role in the quantity of humics that can adsorb to the mineral surface. In addition, recent studies have postulated that the organic coating of clays changes the nature of the mineral surface binding sites for metal contaminants, providing a mechanism for the removal of potentially toxic substances from the environment [32–35].

However, our understanding of the interaction between clays and humic substances, and the effect of humic binding on trace metal sorption by clay mineral surfaces is limited because of our incomplete knowledge of the formation and chemical behavior of humic–clay aggregates and their surfaces. Therefore, the goal of this study is to identify and quantify the reactive functional groups on the kaolinite and illite mineral surfaces responsible for humic acid and trace metal sorption. A discrete site surface complexation modeling approach aided by linear programming optimization (without the need of a pre-defined "initial input guess") was complemented by zeta potential determinations and Fourier transform infrared (FTIR) spectroscopy to account for surface functional groups on clay surfaces upon interaction with peat humic acid (PHA).

2. Materials and methods

2.1. Reagents

Peat humic acid (PHA) was purchased from the International Humics Substances Society (IHSS, USA). Clay minerals (kaolinite KGa-1b and illite Imt-1) were obtained from the Clay Mineral Society Source Clay Repository (University of Missouri, USA). The composition of the kaolinite (KGa-1b) consisted mainly of SiO_2 (44.2%), Al_2O_3 (39.7%) and TiO_2 (1.4%), and the major components of illite (Imt-1) were SiO_2 (49.3%), Al_2O_3 (24.3%) Fe_2O_3 (7.3%) and TiO_2 (0.6%) as described by the source clay physical/chemical data of the Mineral Society Source Clay Repository (University of Missouri, USA). The $CaCl_2$ used in these experiments was 99.99% trace metal basis (Sigma–Aldrich). The surface area of clay minerals was measured by BET, with corresponding values of 9.2 m^2/g and 24.2 m^2/g for kaolinite and illite respectively. The organic matter content in clay minerals was determined to be less than 0.05% using a TOC analyzer (highTOC II, Elementar Analysensysteme GmbH, Hanau, Germany).

2.2. Homoionization of clay minerals

The protocol from Saada et al. (2003) was followed for homoionization of the clay minerals [26]. 0.75 g of clay were shaken (at 150 rpm) with 7.5 mL of 1 M $CaCl_2$ (solid:liquid ratio 1:10) to obtain Ca^{2+}-homoionised kaolinite and illite. This process was repeated three times with 2 h of shaking in between. Excess chloride was removed after the last homoionization step by washing with deionized water until $AgNO_3$ addition to the washing water indicated absence of Cl^{-}.

2.3. Preparation of peat humic acid (PHA) stock solutions

PHA solutions of 0.01 mg/mL (5.5 mg C/L) and 0.1 mg/mL (57.9 mg C/L) were prepared by dissolving 10 and 100 mg of PHA in 1 L deionized water. The pH of the two stock solutions was adjusted to ~7 with 1 M NaOH.

2.4. Preparation of PHA-clay complexes

The Ca^{2+}-homoionized clay was added to the pH-neutral PHA solutions at a ratio of 1:40 (i.e. 0.75 g of dry clay with 30 mL of 0.01 or 0.1 mg/mL PHA). The PHA-clay suspensions were incubated for 48 h at 150 rpm in a horizontal shaker. The suspension was then centrifuged at 5000 rpm for 15 min. The supernatant was sampled for dissolved organic carbon (DOC) measurements to quantify the non-sorbed PHA. To remove loosely bound humics from the PHA-clay, the pellet containing the PHA-clay aggregates was resuspended and gently shaken with deionized water. The suspension was then centrifuged again for at 5000 rpm for 15 min and the supernatant was removed. The supernatant was again sampled for DOC measurements. DOC measurements were carried out by a TOC analyzer (highTOC II, Elementar Analysensysteme GmbH, Hanau, Germany).

2.5. Acid–base titration of clay mineral surfaces

Acid–base titration experiments were conducted at two different calcium chloride concentrations (0.01 and 0.1 M $CaCl_2$), with kaolinite or illite clay, with or without PHA. 0.75 g of clay mineral or PHA-clay aggregates were suspended in 100 mL of the corresponding $CaCl_2$ solution. Aliquots containing 40 mL of suspension were placed inside a Metrohm® glass titration vessel and covered with a Metrohm® lid through which a pH electrode, a custom designed N_2 gas line interface, and a stirrer were fitted. The solution was acidified with 0.01 M HCl to a pH of 4. The pH electrode was calibrated with fresh National Institute of Standards and Technology (NIST) buffer solutions of pH 4.01, 6.86, 9.18 at room temperature, before each experiment. Before the start of the acid–base titration, the system was allowed to reach equilibrium by maintaining a constant pH for a period of 1 h. The pH electrode drift criteria was that the 0.1 M NaOH titrant solution was added only if the change in potential was less than 0.1 mV/min. The titrations were conducted at $4 < pH < 10$ to avoid dissolution of clay minerals.

Previous studies analyzing clay surface acid–base titration data have, for the most part, coupled one or two site pK_a models along with adjustable electrostatic parameters and an *a priori* set of pK_a and site concentration values to provide more flexibility to the optimization of the experimental data fit. In recent works, for example, two site pK_a models have been implemented and com-

bined with electrostatic parameters to fit acid–base titration data arising from the illite surface, as follows:

$$\equiv SOH_2^+ \leftrightarrow \equiv SOH + H^+, Ka_1 \quad (1)$$

$$\equiv SOH \leftrightarrow \equiv SO^- + H^+, Ka_2 \quad (2)$$

where $\equiv SOH_2^+$ and $\equiv SOH$ are considered to be the amphoteric hydroxyl groups from ionized surface sites on the clay mineral surfaces, with their corresponding apparent acidity constants Ka_1 and Ka_2 for the deprotonation reactions at the solid/water interface [6,17,21,22,36–38]. These apparent proton equilibrium constants are usually corrected for electrostatic effects and translated into intrinsic acidity constants through the optimization of an approximate value of the mineral surface charge (Ψ) and the use of electrostatic models, such as the constant capacitance model (CCM) which has been one of the most used routines to describe acid base titration data in the presence of geochemically reactive solids, including mineral surfaces and bacterial cells [21,22,36–38]. This, however, has served to minimize the physico-chemical significance of resulting optimized parameters, as the increased mathematical flexibility of optimization routines, obtained due to the inclusion of electrostatic parameters, permits, almost in all cases, an acceptable fit of experimental data as shown previously [39–41].

In the present study, however, for $j = 1\ldots m$ binding sites on the clay surface, the dissociation mechanism of protons from mineral surface sites is proposed to occur as a combination of j monoprotic reactions:

$$HS_j \xrightarrow{K_a} H^+ + S_j^- \quad (3)$$

where HS_j and S_j^- represent the protonated or deprotonated jth functional group as a function of increasing pH. $K_{a,j}$ is the apparent acidity constant as described below:

$$K_{a,j} = \frac{[S_j^-] \cdot [H^+]}{[HS_j]} \quad (4)$$

where $pK_a = -\log_{10} K_{a,j}$ is a measure of acid strength for each binding site, not yet properly determined for the clay mineral surface.

Therefore apparent pK_a values, embedding electrostatic parameters, and site concentrations on the Ca^{2+}-homoionized clay mineral surface were calculated from the surface charge excess obtained from the raw titration data using:

$$b_{meas,i} = Cb_i - Ca_i + [H^+]_{bulk,i} - [OH^-]_{bulk,i} \quad (5)$$

where $b_{meas,i}$ represents net hydroxide (OH^-) ions consumed by the clay mineral surfaces, Ca_i and Cb_i correspond to the acid and base concentrations respectively at the ith addition of titrant and $[H^+]_{bulk,i}$ and $[OH^-]_{bulk,i}$ denote the concentration of protons and hydroxide in solution calculated from the measured solution pH. Modeling of transformed acid–base titration data was performed using a multi-site Langmuir isotherm approach along with a linear programming optimization method, as described in detail in Kramer et al. [2], Martinez and Ferris [40], Martinez et al. [42], Cox et al. [43].

In order to model transformed acid–base titration data, the surface charge excess, $b_{meas,i}$ in Eq. (5) can be calculated as a function of speciation parameters:

$$b_{calc,i} = \sum_{j=1}^{m} \left(\frac{S_{Tj} K_{a,j}}{K_{a,j} + [H^+]_i} \right) + S_o \quad (6)$$

where S_{Tj} is the concentration of each binding site, and K_{aj} is the acidity constant of each site defined in Eq. (2) as the acid dissociation constant. The constant offset term, S_o, accounts for positive charges on the clay surface. For a true monoprotic system, S_o corresponds to the difference between the sites that are always protonated and those that are always deprotonated over the course of the titration. The model in Eq. (6) was fitted to the experimental data in Eq. (5) using a multi-site Langmuir isotherm and linear programming optimization. No assumptions were made *a priori* regarding the number, pK_a values or concentrations of the deprotonating sites on the clay mineral or on humic-coated clay surfaces [40,42–44].

2.6. Zeta potential measurements

Zeta potentials of Ca^{2+}-homoionized kaolinite and illite clays, in absence or presence of PHA, were measured using a CAD Instrumentation "Zetaphoremeter IV" Z 4000, microelectrophoremeter. Clay suspensions were prepared from previously freeze-dried samples. These solutions were comprised of kaolinite and illite and clay-PHA, with a concentration of 0.01 mg of clay/mL and a 0.01 M $CaCl_2$ concentration. The suspensions were acidified to a pH of 4 with 0.1 M HCl to determine the isoelectric point via interpolation or extrapolation of zeta–pH dependences. The electrophoretic measurements were performed in a quartz cell connecting two Pd electrode chambers. The clay particles were illuminated by a 2 mW He/Ne laser. During the measurements, an electric field of 80 V cm^{-1} was applied in each direction and the images of moving clay particles were transmitted to a computer via a CCD camera. The zeta potential of the clay suspensions was measured by timed image analysis of an average of 20 ± 5 particles for each pH value analyzed. Experiments were performed at pH ranging from 4 to 10.5 with a resolution of 0.3–0.4 pH units. The pH of these suspensions was increased manually by adding 2–10 μL aliquots of 0.1–1 M NaOH. Three replicates were carried out and each was performed with a renewed clay suspension. The uncertainty of zeta potential measurements ranged from 5% to 10%.

2.7. FTIR spectroscopy

All IR spectra were recorded using a Bruker IFS 148 FTIR spectrometer. The spectral resolution of the infrared spectrometer was adjusted to 2 cm^{-1} and 256 interferograms with an optical range from 4000 to 400 cm^{-1} were recorded, both for background and sample measurement. To prepare clay (kaolinite and illite), and PHA-clay samples for FTIR measurement, 2 mg of clay or PHA-clay freeze-dried sample were homogeneously mixed and with 250 mg of dry potassium bromide (KBr – 99.9% Sigma–Aldrich) to prepare a KBr pellet for FTIR measurements. The samples had to be freeze-dried in order to remove water for FTIR measurements, however, slight changes in structure during this procedure cannot be ruled out.

3. Results and discussion

3.1. PHA adsorption to kaolinite and illite

Dissolved organic carbon (DOC) measurements were performed on PHA-clay samples to assess the degree of adsorption of PHA to the kaolinite and illite surfaces under changing conditions of ionic strength and PHA concentration. As shown in Tables 1 and 2, at low PHA concentrations, i.e. 0.01 mg PHA/mL (5.5 mg C/L), the percentage of PHA adsorbed to the mineral surface decreased as the Ca^{2+} concentration increased from 10 to 100 mM. Compared to a maximum PHA sorption to kaolinite of 82% at 10 mM Ca^{2+}, only 74% of the PHA was adsorbed to kaolinite at 100 mM Ca^{2+}. A more pronounced effect was observed for illite (Table 2). In this case, sorption of PHA to the mineral surface decreased from maximum sorption percentages of 79% at 10 mM Ca^{2+} respectively, to 65% at 100 mM. A lower sorption of PHA to the mineral surface may suggest a more open conformation of the PHA molecules [23,26].

Table 1
DOC measurements for 0.01 mg/mL (5.5 mg C/L) and 0.1 mg/mL (57.9 mg C/L) PHA in the presence of kaolinite as a function of increasing Ca^{2+} concentrations.

$[Ca^{2+}]$ (M)	[PHA][a] (mg C/L)	Sorbed [PHA][a] (mg C/L)	% PHA sorbed
0.01	5.5	4.5	82
	5.5	4.4	80
0.1	5.5	4.0	74
	5.5	4.0	73
0.01	57.9	55.8	96
	57.9	55.3	96
0.1	57.9	54.9	95
	57.9	55.3	96

These measurements were carried out at circumneutral pH, and the error in the DOC measurements ranges from 5% to 10%.
[a] [PHA] refers to the concentration of peat humic acid, obtained as described previously.

Table 2
DOC measurements for 0.01 mg/mL (5.5 mgC/L) and 0.1 mg/mL (57.9 mgC/L) PHA in the presence of illite as a function of increasing Ca^{2+} concentrations.

$[Ca^{2+}]$ (M)	[PHA][a] (mg C/L)	Sorbed [PHA][a] (mg C/L)	% PHA sorbed
0.01	5.5	4.3	79
	5.5	4.2	77
0.1	5.5	3.9	71
	5.5	3.6	65
0.01	57.9	54.1	94
	57.9	53.8	93
0.1	57.9	53.8	93
	57.9	53.7	93

These measurements were carried out at circumneutral pH, and the error in the DOC measurements ranges from 5% to 10%.
[a] [PHA] refers to the concentration of peat humic acid, obtained as described previously.

An excess of Ca^{2+}, in the presence of lower PHA concentrations of 0.01 mg/mL (5.5 mg C/L) may imply that sorption occurs through electrostatic attraction of open conformation humic molecules to the clay surface.

At higher PHA concentrations of 0.1 mg/mL (57.9 mg C/L) in the presence of kaolinite and illite (Tables 1 and 2 respectively), more than 95% of the PHA was adsorbed to the kaolinite surface and at least 90% of the PHA was adsorbed to the illite surface for Ca^{2+} concentrations of 10 and 100 mM. The higher sorption of PHA to the kaolinite and illite surfaces at higher PHA concentrations (0.1 mg/mL) and for 10 and 100 mM Ca^{2+} suggests, as mentioned earlier [23,26], that calcium may promote a more compact structure of humic substances. This mechanism, proposed to occur through carboxylate site saturation and intersite bridging by Ca^{2+}, may lead to the changes in PHA conformation required to enhance the quantity of PHA adsorbed to the mineral surface [23,26].

3.2. Acid–base titration of clay and PHA-clay complexes

In order to determine the number and identity of clay surface functional groups and quantify the effects of PHA binding on the clay mineral with respect to surface reactivity, acid base titration experiments were performed. Tables 3–5 present a summary of the results obtained from acid base titration of clay minerals (kaolinite and illite), and PHA-clay complexes. As shown in Table 3, three binding sites were found for both kaolinite and illite mineral phases. For kaolinite, average pK_a values of 4.63 ± 0.07, 8.06 ± 0.07 and 9.38 ± 0.07 were obtained from replicate experiments for Ca^{2+} concentrations of 0.01 and 0.1 M. In the case of illite, complexing sites had pK_a values in the order of 6.39 ± 0.07, 7.90 ± 0.07, and 8.97 ± 0.09 at the same Ca^{2+} concentrations as for kaolinite. Individual fits of pK_a values for both illite and kaolinite were affected

Table 3
Summary of parameters optimized from acid base titration data for kaolinite and illite.

Mineral phase	$[Ca^{2+}]$ (M)	pK_a[a]	SD (μmoles/mg)[b] × 10^{-4}	Total SD[c]
Kaolinite	0.01	4.50 ± 0.07	1.60	5.22
		7.85 ± 0.05	1.13	
		9.15 ± 0.07	2.49	
	0.1	4.75 ± 0.05	1.55	4.36
		8.25 ± 0.07	1.22	
		9.61 ± 0.07	1.59	
Illite	0.01	6.15 ± 0.05	4.29	8.76
		7.65 ± 0.05	2.37	
		8.80 ± 0.05	2.11	
	0.1	6.65 ± 0.05	1.03	4.59
		8.15 ± 0.05	0.91	
		9.15 ± 0.07	2.65	

[a] pK_a is the apparent acid dissociation constant calculated for each site j as described.
[b] SD is the binding site concentration for each site j at the assigned pK_a.
[c] Total SD is the sum of the individual SD values for each site j in Eq. (6).

Table 4
Summary of parameters optimized from acid base titration data for kaolinite in the presence of peat humic acid (PHA).

$[Ca^{2+}]$ (M)	PHA (mg/mL)	pK_a[a]	SD (μmoles/mg) × 10^{-4}[b]	Total SD[c]
0.01	0.01	5.25 ± 0.05	1.03	5.76
		7.10 ± 0.07	1.50	
		8.15 ± 0.09	1.13	
		9.05 ± 0.05	2.11	
	0.1	4.40 ± 0.07	1.43	7.86
		5.31 ± 0.05	1.12	
		6.50 ± 0.07	1.40	
		7.43 ± 0.09	1.33	
		8.78 ± 0.07	2.58	
0.1	0.01	4.75 ± 0.05	1.87	9.49
		6.85 ± 0.07	1.68	
		8.25 ± 0.07	2.45	
		9.55 ± 0.05	3.49	
	0.1	4.60 ± 0.05	1.55	9.33
		5.05 ± 0.07	1.16	
		6.55 ± 0.07	1.73	
		7.55 ± 0.09	1.64	
		8.65 ± 0.07	3.25	

[a] pK_a is the apparent acid dissociation constant calculated for each site j as described.
[b] SD is the binding site concentration for each site j at the assigned pK_a.
[c] Total SD is the sum of the individual SD values for each site j in Eq. (6).

by varying background electrolyte concentration. However, optimized total site concentration ($S_{T,j}$) values in Eq. (6), for illite decreased from 8.76 to 4.59 × 10^{-4} μmoles/mg of clay as a function of increasing Ca^{2+} concentration from 0.01 to 0.1 M. This suggests that the pK_a values are affected by Ca^{2+} concentrations either by electrostatic effects due to increased ionic strength or by Ca^{2+} competition for sorption sites on the clay surface. A similar effect was observed in the case of kaolinite, however, total site concentrations decreased to a lesser extent within the range of 4.36–5.22 × 10^{-4} μmoles/mg of clay (Table 3). This may be explained by the increased electrostatic interaction of background electrolyte cations with the mineral surface as function of ionic strength. This results in a reduced jth binding site concentration available for detection with acid base titration experiments as observed previously for bacterial cell surfaces [39–43].

Because of differences in the clay minerals (kaolinite or illite) in terms of composition, structure and varying acid–base titration

Table 5
Summary of parameters optimized from acid base titration data for illite in the presence of peat humic acid (PHA).

$[Ca^{2+}]$ (M)	PHA (mg/mL)	pK_a[a]	SD (μmoles/mg) × 10^{-4}[b]	Total SD[c]
0.01	0.01	4.45 ± 0.07	2.07	6.45
		6.35 ± 0.09	1.04	
		7.45 ± 0.05	1.46	
		9.05 ± 0.05	1.88	
	0.1	4.15 ± 0.05	2.35	7.37
		5.25 ± 0.05	0.98	
		6.40 ± 0.07	2.04	
		7.75 ± 0.07	1.55	
		8.95 ± 0.07	0.45	
0.1	0.01	4.45 ± 0.05	3.60	9.77
		5.25 ± 0.07	0.82	
		6.45 ± 0.07	1.63	
		8.05 ± 0.07	1.07	
		9.05 ± 0.05	2.65	
	0.1	4.35 ± 0.07	3.91	10.18
		5.85 ± 0.07	1.15	
		6.85 ± 0.05	1.60	
		8.35 ± 0.09	1.52	
		9.35 ± 0.05	2.00	

[a] pK_a is the apparent acid dissociation constant calculated for each site j as described.
[b] SD is the binding site concentration for each site j at the assigned pK_a.
[c] Total SD is the sum of the individual SD values for each site j in Eq. (6).

experiment equilibration times, direct comparison of clay pK_a and total site concentration data with literature values is difficult [38]. However, kaolinite pK_a values form this study are in good agreement with intrinsic and apparent parameters reported by Kramer et al. [2] and Tertre et al. [38] and Wehrli et al. [45]. Average pK_a values of 4.63 ± 0.07 and 8.06 ± 0.07 (Table 3) describe the deprotonation of aluminol ($\equiv AlOH_2^+ \rightarrow \equiv AlOH + H^+$) and silanol ($\equiv SiOH \rightarrow \equiv SiO^- + H^+$) sites at the edge octahedral alumina and silica tetrahedral sheets on kaolinite respectively, whereas the value of 9.38 ± 0.07 is comparable to that reported by Kramer et al. [2], and may provide evidence for a third binding site corresponding to a deprotonation mechanism of AlOH ($\equiv AlOH \rightarrow \equiv AlO^- + H^+$) at alkaline pH [2,38,45]. This suggests a heterogeneous functional group reactivity of the kaolinite surface, and a greater number of surface group ligands available to complex toxic metal cations in soils.

Only a few studies have addressed the illite surface chemistry. These works have relied on one or two pK_a surface complexation models and the FITEQL® optimization routine to quantify the number and concentration of illite surface functional groups [6,11,16,17,20,46]. Acid base titration data, in this study, for Ca^{2+} concentrations of 0.01 and 0.1 M, yielded pK_as of 6.39 ± 0.07 and 8.97 ± 0.09 (Table 3), which suggest the deprotonation of aluminol and silanol groups on the illite surface, as mentioned previously for kaolinite [10–14]. The observed illite pK_a value of 7.90 ± 0.07 is consistent with that reported by Liu et al. 1997 and Du et al. 2001 [16,17]. In their work, however, a three site model was found not to be suitable to describe protonation reactions on the illite surface, as their optimal result set would differ as a function of the initial input guess values of the FITEQL® nonlinear least squares optimization. In this study, however, the multi-site Langmuir isotherm model, was able to establish the presence of a third binding site on the illite surface, therefore, emphasizing the robustness of this semi-empirical model [40,43,44]. The finding of a third reactive site on the clay mineral surface, without the need for prior knowledge of the number or concentration of the sites, may imply a further deprotonation reaction ($AlOH \rightarrow AlO^- + H^+$) on the clay surface, as suggested previously through computer simulation studies of these minerals [10,16–19].

Tables 4 and 5 show the results obtained from the modeling of acid base titration experiments in the presence of kaolinite or illite respectively, and 0.01 or 0.1 mg/mL PHA at Ca^{2+} concentrations of 0.01 and 0.1 M. For kaolinite in the presence of 0.01 mg/mL PHA (Table 4) four binding sites were found with pK_as ranging from 5.25 ± 0.05 to 9.05 ± 0.05 and from 4.75 ± 0.05 to 9.55 ± 0.05 for background electrolyte concentrations of 0.01 and 0.1 M $CaCl_2$ respectively. The average pK_a values observed in Table 4 at 6.98 ± 0.10 and 8.20 ± 0.11, for 0.01 and 0.1 M Ca^{2+} respectively, at 0.01 mg/mL PHA, suggest an additive character to the binding of PHA functional groups to the kaolinite surface. This may indicate a partial sorption of humics to the clay surface, where both functional groups from the mineral and organic fraction could be detected through high resolution acid base titration data analysis, as presented in this study. PHA has been shown to contain carboxylic (—COOH) and phenolic (—OH) groups in different coordination environments, with pK_a values ranging between 4–6, and 9–11 respectively [1,30]. Five binding sites are shown in Table 4 for the kaolinite setups containing 0.1 mg/mL PHA. The presence of the most acidic sites, with average pK_as of 4.40 ± 0.07 and 4.60 ± 0.05 at calcium chloride concentrations of 0.01 and 0.1 M respectively, could be attributed to the adsorption of PHA to the clay mineral surface and subsequent exposure of deprotonating —COOH surface groups. This observation is consistent with the increase in percent of PHA adsorbed on the clay mineral for high ionic strength and PHA concentration, as observed from previous DOC results. Conformational modifications of the PHA molecules upon interaction with dissolved Ca^{2+} have been suggested to increase the quantity of humic acids adsorbing to the clay particle surface [23,26], however, in addition, the presence of Ca^{2+} may lead to bridging of clay and humic functional groups, and to the condensation/aggregation of humic molecules.

Table 5 shows the optimized binding site concentrations, along with their corresponding pK_a values for illite in the presence of 0.01 and 0.1 mg/mL PHA, and varying Ca^{2+} concentration. Four or five binding sites were obtained for background electrolyte concentrations of 0.01 and 0.1 M Ca^{2+} respectively, with total number and concentration of binding sites increasing proportionally as a function of PHA concentration (Table 5). The presence of five binding sites is indicative of exposed PHA functional groups on the clay surface. This is indicative of an additive nature of the PHA adsorption on the clay mineral surface. This is suggested by the increase in total binding site concentration observed in Tables 4 and 5 for PHA-coated kaolinite and illite respectively, as described previously for bacteriogenic iron oxides [47,48]. At high calcium chloride concentrations and high PHA concentration, the interaction of PHA molecules with background electrolytes, Ca^{2+}, may increase the quantity of PHA adsorbed on the clay surface and therefore the binding site concentration [23,26].

Individual and total binding site concentrations are reported in Tables 3–5 for kaolinite and illite, as well as for PHA-coated clay mineral in the presence of 0.01 or 0.1 mg/mL PHA. The three sites reported in Table 1 for kaolinite at 0.01 and 0.1 M $CaCl_2$, show decreasing total site concentrations of 5.22 and 4.36×10^{-4} μmol/mg clay respectively. Similarly for illite, decreasing values of total binding site concentrations were observed at 8.76 and 4.59×10^{-4} μmoles/mg clay for the increasing concentrations of 0.01 and 0.1 M $CaCl_2$. Tables 4 and 5 show variations of the total complexing site density as a function of increasing PHA and background electrolyte concentrations. In general for both kaolinite and illite total binding site concentrations increase to maximum values of 9.33 and 10.18×10^{-4} μmol/mg clay, respectively at conditions of high PHA concentration (0.1 mg/mL) and 0.1 M $CaCl_2$. A similar increase in site density concentration is also observed for the lower

PHA concentration from 5.76 to 9.49, and 6.45 to 9.77 μmol/mg clay, for kaolinite and illite respectively (Tables 4 and 5). This is indicative of an enhancement of PHA adsorption to the clay mineral surface with increasing background electrolyte concentration as confirmed by DOC analysis, and may also suggest changes in PHA molecule conformation at higher Ca^{2+} concentrations as suggested previously [23,26]. As mentioned earlier, a higher background electrolyte concentration, given by increasing Ca^{2+} in this study, may cause humic molecules to condense and sorb to the mineral surface, increasing the total binding site concentration. From the site density values in Tables 3–5, an additive, rather than a masking of clay surface functional groups could be inferred [23,26].

3.3. Zeta potential measurements of clay and PHA-clay suspensions

Zeta potential measurements of clay suspensions (kaolinite or illite) in the presence and absence of PHA indicate the development of a net particle negative surface charge as a function of increasing pH. Fig. 1 presents zeta potentials measured for Ca^{2+}-homoionized kaolinite, and for PHA-kaolinite complexes at a concentration of 0.01 M Ca^{2+}.

The zeta potential values shown for kaolinite were obtained in the pH range of 4–10. Those contained in the pH range of 4–7, show a general decrease in surface potential with increasing pH, as shown from the initial value of −30.1 ± 5.8 mV at pH 4.4 to that of −36.1 ± 1.6 mV at pH 6.6. This is consistent with the result obtained previously for kaolinite where a single acidic site was available to undergo deprotonation reactions at a $pK_a \sim 4.6$. At pH 7, a drop in surface potential, to −50.8 ± 3.0 mV, is observed, suggesting the deprotonation of a further available surface site as shown in Table 1. The surface potential then decreases only slightly to reach a value of −53.2 ± 6.6 mV at pH 9.1. Further measurements of zeta potential values for kaolinite, within the pH range of 9.1–10.4, show increasing surface potentials which scale up from −47.8 ± 2.2 to a maximum of −42.1 ± 2.8 mV at pH 10.4. This increase in potential to more positive values for kaolinite at alkaline pH, may suggest the further deprotonation of AlOH groups as described earlier and the electrostatic interaction of background Ca^{2+} electrolyte cations. This effect should be able to generate a more apparent positive charge on the clay mineral surface.

Fig. 1 shows, in addition, the results of measured zeta potential values for kaolinite in the presence of 0.1 mg/mL PHA and a background electrolyte concentration of 0.01 M Ca^{2+}. The zeta potential values obtained in the presence of PHA are more negative than those for the clay mineral phase. From an initial potential of −54.3 ± 4.1 mV at pH 4.5, surface potential values of −57.2 ± 3.7, −60.8 ± 3.1, −63.1 ± 5.9 and −60.5 ± 3.8 mV were recorded at pH 5.7, 6.8, 8.8 and 10.4 respectively. This confirms an enhanced negative surface charge on the PHA-coated kaolinite surface and further emphasize the ability of humic substances to sorb to the clay mineral surface. An electrostatic interaction of organic carboxylate functional groups with the clay surface can be inferred from the more negative zeta potentials measured for the PHA-kaolinite sample as a function of increasing pH. At alkaline pH values, functional groups in humic acid (e.g. phenolic groups) would deprotonate and further interact with background electrolyte cations giving rise to a less negative particles surface potential (Fig. 1). The lower potential observed at pH 10.4 for PHA-kaolinite compared to kaolinite may indicate the deprotonation of high pK_a humic surface functional groups.

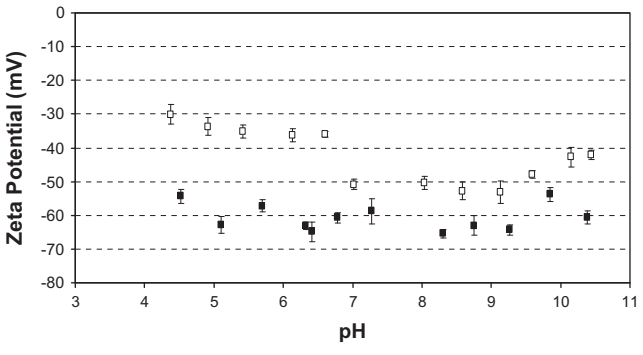

Fig. 1. Measured zeta potential of kaolinite (□) and PHA-kaolinite (■) in the pH range of 4 < pH < 10.5 and the kaolinite or PHA-kaolinite concentrations used were in the order of 0.01 mg/mL, in 0.01 M $CaCl_2$ as the background electrolyte.

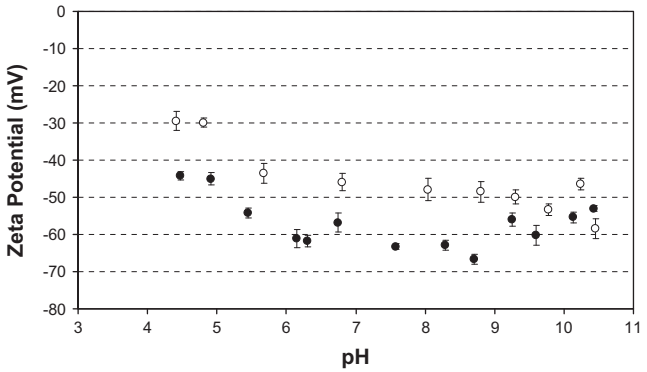

Fig. 2. Measured zeta potential of illite (○) and PHA-illite (●) in the pH range of 4 < pH < 10.5 and the illite or PHA-illite concentrations used were in the order of 0.01 mg/mL in 0.01 M $CaCl_2$ as the background electrolyte.

Fig. 2 shows the results of zeta potential measurements for illite in absence and presence of 0.1 mg/mL PHA respectively.

These measurements were recorded at a concentration of 0.01 M Ca^{2+}. Values for illite alone show a decrease in surface potentials in the pH range of 4.4–10.4. An initial zeta potential of −29.5 ± 2.4 mV was recorded at a pH of 4.4. A decrease in potential occurs at a pH of 5.7 to −43.5 ± 4.6 mV. This drop in potential is consistent with the deprotonation of the most acidic site for the illite surface, reported in Table 1, with a pK_a of ~6.2. Significant differences are observed in the illite and PHA-illite zeta potential values in the range of pH 4–9. No significant differences in the zeta potential values are observed for illite in Fig. 2 at alkaline pH values higher than 9. The observation of a more negative potential suggests the complexation of humics to the illite surface, as described previously for kaolinite.

Zeta potential values for illite in the presence of PHA, also described in Fig. 2, confirm the interaction of organic matter with the mineral surface. An initial potential of −44.2 ± 2.3 mV was measured for illite at pH 4.5. The surface potential for this mineral decreased to −54.2 ± 2.6 mV at a pH of 5.6, suggesting the presence of a weakly acidic site on the illite surface, as mentioned previously. Values of zeta potential fluctuate within the narrow range of −60 to −65 mV in the pH range of 5.6–10.4, as shown in Fig. 2. This fluctuation represents an approximate decrease of 20 mV in the presence of PHA. This implies a similar effect of humic substance adsorption to the illite mineral surface, as that described previously for kaolinite-humics systems. Comparison of zeta potentials from pure mineral phases and PHA-bound clays show a general decrease of surface charge in the presence of PHA. This effect may be attributed to the interaction of humic substances with deprotonated aluminol and silanol functional groups on the clay surface, as suggested previously [5,27,49,50].

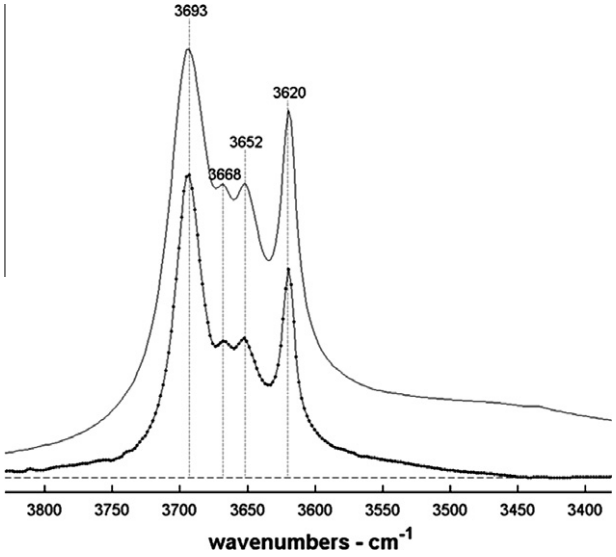

Fig. 3a. Dotted and solid lines represent Fourier transform infrared (FTIR) spectra of kaolinite and PHA-kaolinite respectively depicting absorbance values ranging from 4000 to 3400 cm^{-1}. These peaks are characteristic of kaolinite as described previously.

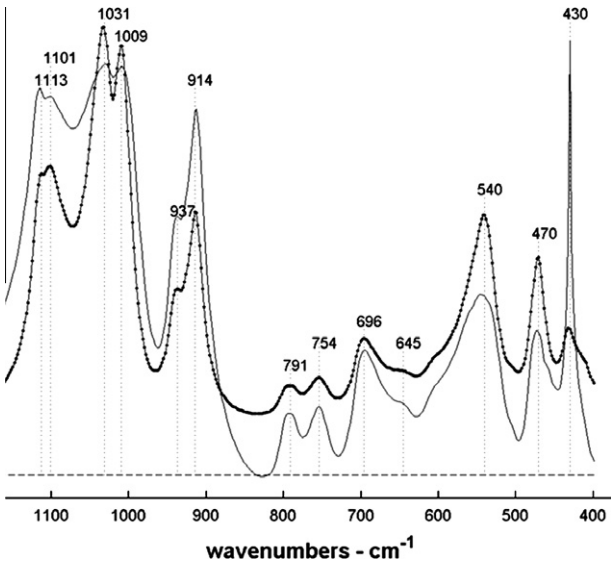

Fig. 3b. Dotted and solid lines represent Fourier transform infrared (FTIR) spectra of kaolinite and PHA-kaolinite respectively depicting absorbance values ranging from 1200 to 400 cm^{-1}. These peaks are characteristic of kaolinite as describe previously.

3.4. FTIR spectroscopy of clays and PHA-clay

Figs. 3a–3c show FTIR spectra measured for kaolinite (dotted lines) and PHA-kaolinite complexes (solid lines).

Absorbance values, in Fig. 3a at 3693, 3668, 3652 and 3620 cm^{-1} for both kaolinite and PHA-kaolinite complexes have been assigned to stretching and vibrational modes of kaolinite [10,12,51]. The band observed at 3693 cm^{-1} has been previously shown to represent the Al···O—H stretching vibration mode of "inner surface hydroxyls" located at the surface of octahedral sheets opposite to tetrahedral oxygens of the adjacent kaolinite layer [10,12,51]. The band at 3620 cm^{-1}, in Fig. 3a, coincides with that of "inner hydroxyls" located on the plane, common to octahedral and tetrahedral sheets, as described previously. Bands recorded at 3668 and 3652 cm^{-1} are suggested to emerge from the vibration

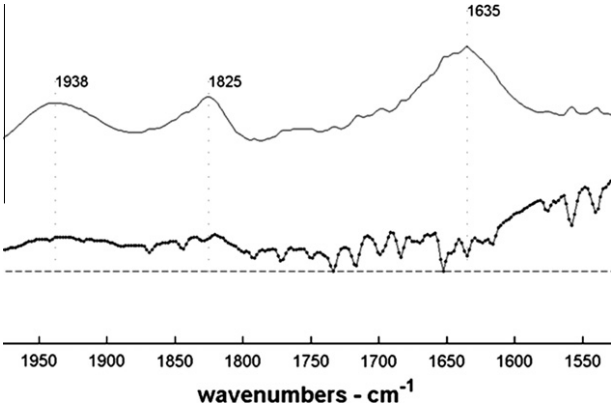

Fig. 3c. Dotted and solid lines represent Fourier transform infrared (FTIR) spectra of kaolinite and PHA-kaolinite respectively depicting absorbance values ranging from 2000 to 1500 cm^{-1}. These weak absorbance peaks, present only in PHA-kaolinite systems, should correspond to amine (—NH_2) or carbonyl (>C=O) vibrations.

Table 6
Main IR Absorption bands from the normalized difference spectrum from PHA-kaolinite and kaolinite spectra.[a]

Frequency (cm^{-1})	Assignment[b]
3440	O—H stretching, trace N—H stretching
2930	Aliphatic C—H stretching
2361	Bands at 2361 and 2335 cm^{-1}: OH stretching from COOH
2335	
1652	C=O stretching of COOH and trace ketones
1646	C=O stretching of amide groups (amide I band) and/or
1635	quinone C=O

[a] Spectra for the mineral phases (kaolinite and illite) were normalized to those of PHA-kaolinite and PHA-illite spectra.
[b] Frequency bands in Tables 4 and 5 were assigned according to those described in reference [1,51,52].

of "outer hydroxyls" located at the surface and along broken edges of kaolinite monocrystals [10,12,51]. In Fig. 3b absorption bands at 1113 and 1101 cm^{-1} are associated with Si—O stretching vibrations, while those at 1031 and 1009 cm^{-1} are characteristic of Si—O—Si and Si—O—Al lattice vibrations [10,12,51,52]. Further bands at 937 and 914 cm^{-1} in Fig. 3b can be attributed to "inner surface hydroxyls" and "inner hydroxyls" respectively mainly caused by Al—OH groups. Fig. 3b represents the bands at lower frequency wavenumbers (ranging from 1200 to 400 cm^{-1}). These absorbance values confirm the presence of a Si-translation (791 cm^{-1}), a Si—O stretch (754 and 696 cm^{-1}), an Al—O stretch (645 cm^{-1}). Bending vibrations of Si—O and Si—O—Al were found at 540, and 470 cm^{-1}, as reported earlier for kaolinite [10,12,51]. The absorbance value at 430 cm^{-1} corresponds to the OTO (O—Al—O) bend in the kaolinite [10,12,51,52].

The solid lines in Figs. 3a–3c correspond to the FTIR vibrational frequencies of PHA-coated kaolinite. All absorption bands previously described for kaolinite are present in the PHA-kaolinite spectrum (in Figs. 3a–3c). However, in addition, weak absorption bands characteristic of PHA sorbed to kaolinite (Fig. 3c), were observed at 1938, 1825 and 1635 cm^{-1}. The absorption band at 1938 cm^{-1} suggests the presence of amino acids or amine groups, while the band at 1825 cm^{-1} suggests the presence of C—H vibrations or an anhydrous carbonyl (C=O) stretch. The absorption frequency observed at 1635 cm^{-1} indicates an H—O—H stretch suggesting water sorption to the mineral surface [1,53,54]. Further indication of PHA kaolinite surface interaction arises from the calculated difference spectrum frequencies in Table 6. In order to substract the PHA-kaolinite form the kaolinite mineral spectrum, data from the PHA

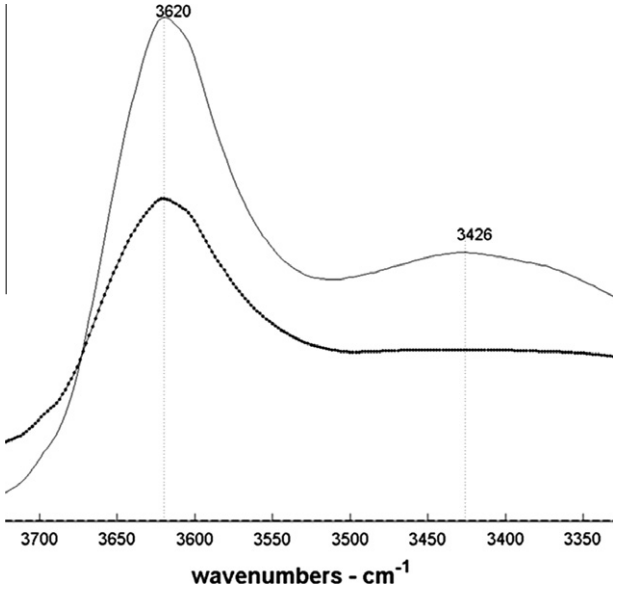

Fig. 4a. Dotted and solid lines represent Fourier transform infrared (FTIR) spectra of kaolinite and PHA-illite respectively depicting absorbance values ranging from 4000 to 3300 cm^{-1}. These peaks are characteristic of illite as described previously.

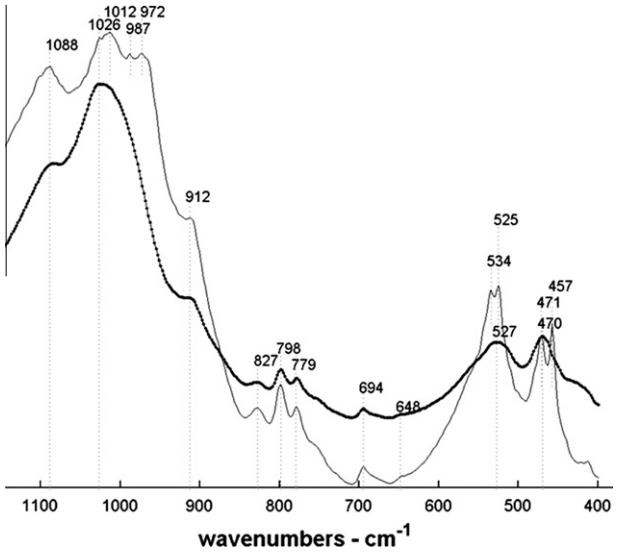

Fig. 4b. Dotted and solid lines represent Fourier transform infrared (FTIR) spectra of illite and PHA-illite respectively depicting absorbance values ranging from 1200 to 400 cm^{-1}. These peaks are characteristic of illite as describe previously.

containing spectrum was normalized to the highest absorbance value in the kaolinite spectrum and the data multiplied by the ratio obtained for the same peak at a particular wavenumber value. These procedure generated absorption bands for the PHA-kaolinite system. Main absorption bands indicating the presence of PHA appear at vibrational frequencies of —CH_2— and —CH_3— structures in humic substances (2920 and 2950 cm^{-1} respectively), and most importantly from —COOH at 2966 cm^{-1} (Table 4) [1,55].

FTIR spectra for illite (dotted lines) and PHA-illite (solid lines) are shown in Figs. 4a–4c.

The main features of the illite spectral data, in Fig. 4a, ranging from 4000 to 3300 cm^{-1}, indicate main vibrational frequencies at 3620 and 3426 cm^{-1} corresponding to Al···O—H stretch vibrations and H—O—H respectively, for bound water and Al_2OH on illite. Fig. 4b shows absorbance bands for illite and PHA-illite in the

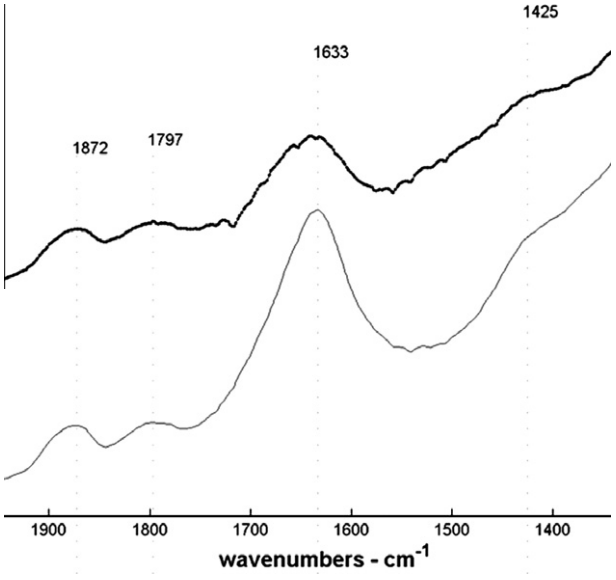

Fig. 4c. Dotted and solid lines represent Fourier transform infrared (FTIR) spectra of illite and PHA-illite respectively depicting absorbance values ranging from 2000 to 1500 cm^{-1}. These weak absorbance peaks shown, may correspond to amine (—NH_2) or carbonyl (>C═O) vibrations, as well as that of water at 1635 cm^{-1}. These peaks could indicate the presence of PHA on the illite surface, as explained in text.

Table 7
Main IR Absorption bands from the normalized difference spectrum from PHA-illite and illite spectra.[a]

Frequency (cm^{-1})	Assignment[b]
3427	O—H stretching, trace N—H stretching
2931	Aliphatic C—H stretching
2856	Bands at 2361 and 2335 cm^{-1}: OH stretching from
2362	COOH
2338	
1716	C═O stretching of COOH and trace ketones
1635	C═O stretching of amide groups (amide I band) and/or quinone C═O
1363	OH deformation and C—O stretching of phenolic OH C—H deformation of CH_2 and CH_3 groups COO^- antisymmetric stretching

[a] Spectra for the mineral phases (kaolinite and illite) were normalized to those of PHA-kaolinite and PHA-illite spectra.
[b] Frequency bands in Tables 4 and 5 were assigned according to those described in reference [1,51,52].

range of 1200–400 cm^{-1}. Wavenumbers extending from 1088 to 972 cm^{-1} correspond to separate Si—O absorptions. The value of 912 cm^{-1}, has been previously reported as characteristic of the presence of illite, as an Al_2OH in-plane vibration band [10,52,56,57]. Wavenumbers in the range of 850–400 cm^{-1}, show an absorption band at 470 cm^{-1} which can be attributed to a Si—O stretch, while that at 527 cm^{-1} results from an Si—O bending mode vibration, in combination with vibrational frequency values of 827, 798, 779 and 694 cm^{-1}. The absorption band at 648 cm^{-1} suggests the presence of iron rich chlorites [10,52,56,57].

The solid line spectra in Figs. 4a–4c, represent those of PHA-coated illite. In addition to the vibrational frequencies described above for the mineral phase, these spectra may suggest characteristic vibrations expected for peat humic acids. These were obtained from the analysis of vibrational frequencies in Fig. 4c and the difference spectrum calculated from the subtraction of illite and normalized PHA-illite spectra (Table 7). Spectra were normalized as

described previously for kaolinite. Absorbance values at 1872, 1797 and 1425 cm^{-1} may arise from sorption of PHA to illite. The absorbance band at 1425 cm^{-1} suggests, for example, bending vibrations of aliphatic C—H. This is unclear, however, as these absorbances are present in both the illite and the PHA-illite spectra (Fig. 4c). The absorbance band at 1633 cm^{-1} (Fig. 4c) represents water adsorption on the mineral surface. From the calculated difference spectra in Table 7, the PHA-illite mineral phase interactions may be inferred from the presence of weak absorption bands, characteristic of organic matter, ranging from 3427 to 1363 cm^{-1} [1,53,54].

4. Conclusions

The use of dissolved organic carbon measurements, acid–base titrations, flexible surface complexation models, zeta potential and infrared spectroscopic data demonstrated PHA adsorption to the clay mineral surface and an increase in the number and concentration of surface sites available for deprotonation and potential sorption of toxic metal cations. The increase in the number of surface functional groups and the increase in surface site concentration, suggest an additive character, rather than a masking of clay surface groups by sorbed humics. Zeta potential measurements were able to confirm a more negative surface charge in the presence of organic matter, attributed to the sorption of PHA on the clay surface as a function of increasing pH. The presence of humic substance interaction with the clay mineral surface was strongly suggested from the analysis of FTIR spectroscopic data.

Acknowledgments

This work was supported by an Alexander von Humboldt Foundation Experienced Researcher Fellowship to REM, an IPSWaT Doctoral Fellowship awarded to PS, and BMBF support to AK. The authors thank Johannes Ofner from the Forschungsstelle Atmosphärische Chemie, Universität Bayreuth, Germany for FTIR measurement of clay samples, Dr. Oleg S. Pokrovsky of the CNRS-OMP-LMTG in Toulouse, France, for the time made available to use the zeta potential instrument in his laboratory. In addition Dr. Martin Obst, Dr. Christian Schröder, and Florian Hegler are thanked for their helpful comments during the preparation of this manuscript.

References

[1] F.J. Stevenson, Humus Chemistry: Genesis, Composition, Reactions, John Wiley & Sons, New York, 1994.
[2] J.R. Kramer, P. Collins, P. Brassard, Mar. Chem. 36 (1991) 1.
[3] I. Sondi, V. Pravdić, Croat. Chem. Acta 71 (1998) 1061.
[4] E. Tombácz, Z. Libor, E. Illés, A. Majzik, E. Klumpp, Org. Geochem. 35 (2004) 257.
[5] R. Kretzschmar, D. Hesterberg, H. Sticher, Soil Sci. Soc. Am. J. 61 (1997) 101.
[6] G. Sposito, N.T. Skipper, R. Sutton, S. Park, A.K. Soper, J.A. Greathouse, Proc. Natl. Acad. Sci. U. S. A. 96 (1999) 3358.
[7] U. Neubauer, B. Nowack, G. Furrer, R. Schulin, Environ. Sci. Technol. 34 (2000) 2749.
[8] S.M.I. Sajidu, I. Persson, W.R.L. Masamba, E.M.T. Henry, J. Hazard. Mater. 158 (2008) 401.
[9] G.C. Gupta, F.L. Harrison, Water Air Soil Pollut 17 (1982) 357.
[10] D. Bougeard, K.S. Smirnov, E. Geidel, J. Phys. Chem. B 104 (2000) 9210.
[11] K.L. Konan, C. Peyratout, J.-P. Bonnet, A. Smith, A. Jacquet, P. Magnoux, P. Ayrault, J. Colloid Interface Sci. 307 (2007) 101.
[12] J. Kristóf, R.L. Frost, A. Felinger, J. Mink, J. Mol. Struct. 410–411 (1997) 119.
[13] J.E. Thomas, M.J. Kelley, J. Colloid Interface Sci. 322 (2008) 516.
[14] J.C. Miranda-Trevino, C.A. Coles, Appl. Clay Sci. 23 (2003) 133.
[15] C. Ma, R.A. Eggleton, Clays Clay Miner. 47 (1999) 174.
[16] W. Liu, Water Res. 35 (2001) 4111.
[17] Q. Du, Z. Sun, W. Forsling, H. Tang, J. Colloid Interface Sci. 187 (1997) 221.
[18] S. Ferrari, A.F. Gualtieri, G.H. Grathoff, M. Leoni, Z. Kristallogr. (Suppl. 23) (2006) 493.
[19] C. Tao, W. HeJing, Sci. China Ser. D – Earth Sci. 50 (2007) 1452.
[20] J.C. Westall, FITEQL: A Computer Program for Determination of Chemical Equilibrium Constants from Experimental Data, Report 82-01. Department of Chemistry, Oregon State University, Corvallis, OR, 1982.
[21] P. Leroy, A. Revil, J. Colloid Interface Sci. 270 (2004) 371.
[22] B.K. Schroth, G. Sposito, Clays Clay Miner. 45 (1997) 85.
[23] E.M. Murphy, J.M. Zachara, Geoderma 67 (1995) 103.
[24] M. Rebhun, R. Kalabo, L. Grossman, J. Manka, Ch. Rav-Acha, Water Res. 26 (1992) 79.
[25] M. Meier, K. Namjesnik-Dejanovic, P.A. Maurice, Y.-P. Chin, G.R. Aiken, Chem. Geol. 157 (1999) 275.
[26] A. Saada, H. Gaboriau, S. Cornu, F. Bardot, F. Villiéras, J.P. Croué, Clay Miner. 38 (2003) 433.
[27] G.U. Balcke, N.A. Kulikova, S. Hesse, F.-D. Kopinke, I.V. Perminova, F.H. Frimmel, Soil Sci. Soc. Am. J. 66 (2002) 1805.
[28] M.B. Hay, S.C.B. Myneni, Geochim. Cosmochim. Acta 71 (2007) 3518.
[29] L. Li, W. Huang, P. Peng, G. Sheng, J. Fu, Soil Sci. Soc. Am. J. 67 (2003) 740.
[30] W. Stumm, J.J. Morgan, Aquatic Chemistry: Chemical Equilibria and Rates in Natural Waters, John Wiley & Sons, New York, 1996.
[31] G.H. Bolt, B.P. Warkentin, Kolloid-Zeitschrift 156 (1957) 41.
[32] S. Nir, Soil Sci. Soc. Am. J. 50 (1986) 52.
[33] T. Polubesova, S. Nir, Clays Clay Miner. 47 (1999) 366.
[34] B.L. Sawhney, Clays Clay Miner. 20 (1972) 93.
[35] O.L. Gaskova, M.B. Bukaty, Phys. Chem. Earth 33 (2008) 1050.
[36] S.A. Hussain, Ş. Demirci, G. Özbayoğlu, J. Colloid Interface Sci. 184 (1996) 535.
[37] M. Tschapek, L. Tcheichvili, C. Wasowski, Clay Miner. 10 (1974) 219.
[38] E. Tertre, S. Castet, G. Berger, M. Loubet, E. Giffaut, Geochim. Cosmochim. Acta 70 (2006) 4579.
[39] D.S. Smith, F.G. Ferris, Methods Enzymol. 337 (2001) 225.
[40] R.E. Martinez, F.G. Ferris, J. Colloid Interface Sci. 243 (2001) 73.
[41] R.E. Martinez, D.S. Smith, E. Kulczycki, F.G. Ferris, J. Colloid Interface Sci. 253 (2002) 130.
[42] R.E. Martinez, K. Pedersen, F.G. Ferris, Interface Sci. 275 (2004) 82.
[43] J.S. Cox, D.S. Smith, L.A. Warren, F.G. Ferris, Environ. Sci. Technol. 33 (1999) 4514.
[44] P. Brassard, J.R. Kramer, P.V. Collins, Environ. Sci. Technol. 24 (1990) 195.
[45] B. Wehrli, E. Wieland, G. Furrer, Aquat. Sci. 52 (1990) 1.
[46] X. Gu, L.J. Evans, Geochim. Cosmochim. Acta 72 (2008) 267.
[47] A.W.P. Vermeer, J.K. McCulloch, W.H. Van Riemsdijk, L.K. Koopal, Environ. Sci. Technol. 33 (1999) 3892.
[48] R.E. Martinez, D.S. Smith, K. Pedersen, F.G. Ferris, Environ. Sci. Technol. 37 (2003) 5671.
[49] E. Ghabbour, G. Davies, M.E. Goodwillie, K. O'Donaughy, T.L. Smith, Environ. Sci. Technol. 38 (2004) 3338.
[50] S. Kang, B. Xing, Langmuir 23 (2007) 7024.
[51] M. Hoch, A. Bandara, Colloids Surf., A: Physicochem. Eng. Aspects 253 (2005) 117.
[52] K. Oinuma, H. Hayashi, Am. Mineral. 50 (1965) 1213.
[53] G. Jalovszky, S. Holly, M. Hollósi, J. Mol. Struct. 348 (1995) 329.
[54] L.O.B. Benetoli, C.M.D. de Souza, K.L. da Silva, I.G. de Souza Jr., H. de Santana, A. Paesano Jr., A.C.S. da Costa, C.T.B.V. Zaia, D.A.M. Zaia, Origins Life Evol. Biosph. 37 (2007) 479.
[55] M. Tatzber, M. Stemmer, H. Spiegel, C. Katzlberger, G. Haberhauer, A. Mentler, M.H. Gerzabek, J. Plant Nutr. Soil Sci. 170 (2007) 522.
[56] J. Pironon, M. Pelletier, P. de Donato, R. Mosser-Ruck, Clay Miner. 38 (2003) 201.
[57] J.L. Post, L. Borer, Appl. Clay Sci. 22 (2002) 77.